Published in final edited form as:
Nat Genet. 2015 June ; 47(6): 579–581. doi:10.1038/ng.3289.

Mutations in *XPR1* cause primary familial brain calcification associated with altered phosphate export

Andrea Legati[1,§], **Donatella Giovannini**[2,3,4,§], **Gaël Nicolas**[5,6], **Uriel López-Sánchez**[2,3,4], **Beatriz Quintáns**[7], **João Oliveira**[8], **Renee L. Sears**[1,27], **Eliana Marisa Ramos**[1], **Elizabeth Spiteri**[9,28], **María-Jesús Sobrido**[7], **Ángel Carracedo**[7], **Cristina Castro-Fernández**[7], **Stéphanie Cubizolle**[10], **Brent L. Fogel**[9], **Cyril Goizet**[11], **Joanna C. Jen**[9], **Suppachok Kirdlarp**[12], **Anthony E. Lang**[13], **Zosia Miedzybrodzka**[14], **Witoon Mitarnun**[12], **Martin Paucar**[15], **Henry Paulson**[16], **Jérémie Pariente**[17], **Anne-Claire Richard**[5], **Naomi S. Salins**[18], **Sheila A. Simpson**[14], **Pasquale Striano**[19], **Per Svenningsson**[15], **François Tison**[10], **Vivek K. Unni**[20], **Olivier Vanakker**[21], **Marja W. Wessels**[22], **Suppachok Wetchaphanphesat**[12], **Michele Yang**[23], **Francois Boller**[24], **Dominique Campion**[5,25], **Didier Hannequin**[5,6,26], **Marc Sitbon**[2,3,4], **Daniel H. Geschwind**[1,9], **Jean-Luc Battini**[2,3,4], and **Giovanni Coppola**[1,9]

[1]Department of Psychiatry, David Geffen School of Medicine, University of California Los Angeles, Los Angeles, CA, USA [2]Institut de Génétique Moléculaire de Montpellier, CNRS UMR5535, Montpellier, France [3]Université de Montpellier, F-34293 Cedex 5, Montpellier, France [4]Laboratories of Excellence GR-Ex, Paris and EpiGenMed, Montpellier, France [5]Inserm U1079, IRIB, University of Rouen and CNR-MAJ, Rouen University Hospital, Rouen, France [6]Department of Genetics, Rouen University Hospital, Rouen, France [7]Fundación Pública Galega de Medicina Xenómica-SERGAS-IDIS (Hospital Clínico Universitario) and Grupo de Medicina Xenómica-

Corresponding authors: Jean-Luc Battini, PhD, Directeur de Recherche INSERM, Institut de Génétique Moléculaire de Montpellier, CNRS UMR 5535, 1919, route de Mende, 34293 Montpellier Cedex 05 - France, Tel: +33 (0)4 34 35 96 40, Fax: +33 (0)4 34 35 96 34, jean-luc.battini@igmm.cnrs.fr, Giovanni Coppola, MD, Semel Institute for Neuroscience and Human Behavior, Departments of Psychiatry & Neurology, David Geffen School of Medicine, #3506C Gonda Neuroscience and Genetics Research Center, University of California Los Angeles, 695 Charles E. Young Dr. South, Los Angeles, CA 90095, Tel: (310) 794-4172, Fax: (310) 794-9613, gcoppola@ucla.edu.
[§]equal contribution
[27]Current address: Department of Genetics, Center for Genome Sciences and Systems Biology, Washington University School of Medicine, St. Louis, MO, USA
[28]Current address: Kaiser Permanente, Southern California Permanente Medical Group, Regional Reference Laboratories, Genetics Laboratory, Los Angeles, CA, USA

URLs
Allen Mouse Brain Atlas database, http://mouse.brain-map.org
TOPO2 Transmembrane protein display software, http://www.sacs.ucsf.edu/TOPO2
dbSNP database, http://www.ncbi.nlm.nih.gov/SNP
1000 Genomes Project, http://www.1000genomes.org
Exome Variant Server, http://evs.gs.washington.edu/EVS

Author Contributions
M.S., D.H.G., J.-L.B., G.C. designed the study; A.L., D.G., G.N., U.L.-S. designed and performed experiments; A.L., D.G., G.N., U.L.-S., B.Q., J.O., R.S., E.M.R., E.S., M.-J.S., A.-C.R., D.C., M.S., D.H.G., J.-L.B., G.C. analyzed data; A.L., D.G., M.S., J.-L.B., G.C. wrote the manuscript; A.L., D.G., G.N., J.O., R.S., E.M.R., M.-J.S., B.L.F., A.E.L., Z.M., H.P., P.S., V.K.U., M.W.W., M.S., J.-L.B., G.C. edited the manuscript; G.N., B.Q., J.O., E.S., M.-J.S., A.C., C.C.-F., S.C., B.L.F., C.G., J.C.J., S.K., A.E.L., Z.M., W.M., M.P., H.P., J.P., N.S.S., S.A.S., P.S., P.S., F.T., V.K.U., O.V., M.W.W., S.W., M.Y., F.B., D.H., D.H.G., G.C. recruited and evaluated patients, and collected blood samples.

CIBERER (Universidad de Santiago de Compostela). Santiago de Compostela, Spain [8]Keizo Asami Laboratory, Federal University of Pernambuco, Recife, Brazil [9]Department of Neurology, David Geffen School of Medicine, University of California Los Angeles, Los Angeles, CA, USA [10]Neurology and Institute for Neurodegenerative diseases, Bordeaux University Hospital, and Bordeaux University, France [11]Unité de Génétique Médicale, Bordeaux Hospital University Center, Bordeaux, France [12]Division of Medicine, Buriram Hospital, Buriram, Thailand [13]The Morton and Gloria Movement Disorders Clinic and the Edmond J. Safra Program in Parkinson's Disease, Toronto Western Hospital, Toronto, Canada [14]Medical Genetics Group, School of Medicine & Dentistry, University of Aberdeen, Polwarth Building, Foresterhill, Aberdeen, UK AB25 2ZD [15]Translational Neuropharmacology, Clinical Neuroscience, Center for Molecular Medicine, Karolinska Institute and Department of Neurology, Karolinska Hospital, Huddinge, Stockholm, Sweden [16]Department of Neurology, University of Michigan, Ann Arbor, MI, USA [17]INSERM, Imagerie Cérébrale et Handicaps Neurologiques, Centre Hospitalier Universitaire de Toulouse, UMR 825, Pole Neurosciences, CHU Purpan, place du Dr Baylac, F-31059 Toulouse, France; Université de Toulouse, UPS, Toulouse, France [18]Barrow Neurological Institute, Phoenix, AZ, USA [19]Pediatric Neurology and Muscular Diseases Unit, Department of Neurosciences, Rehabilitation, Ophthalmology, Genetics, Maternal and Child Health, University of Genoa, "G. Gaslini" Institute, Genova, Italy [20]Department of Neurology, Oregon Health & Science University, Portland, OR, USA [21]Center for Medical Genetics, Ghent University Hospital, De Pintelaan 185, B-9000 Ghent, Belgium [22]Department of Clinical Genetics, Erasmus Medical Center, Rotterdam, The Netherlands [23]Department of Pediatrics, Children's Hospital Colorado and the University of Colorado Denver, Aurora, CO, USA [24]Department of Neurology, George Washington University Medical School, Washington, DC, USA [25]Department of Research, Rouvray Psychiatric Hospital, Sotteville-lès-Rouen, France [26]Department of Neurology, Rouen University Hospital, Rouen, France

Abstract

Primary familial brain calcification (PFBC) is a neurological disease characterized by calcium phosphate deposits in the basal ganglia and other brain regions, thus far associated with *SLC20A2*, *PDGFB*, or *PDGFRB* mutations. We identified in multiple PFBC families mutations in *XPR1*, a gene encoding a retroviral receptor with phosphate export function. These mutations alter phosphate export, providing a direct evidence of an impact of *XPR1* and phosphate homeostasis in PFBC.

PFBC, also known as idiopathic basal ganglia calcification, or Fahr's disease, is a rare, clinically heterogeneous neurodegenerative disorder[1]. PFBC symptoms typically occur after the age of 40, with progressive neuropsychiatric and movement disorders, although some individuals may remain asymptomatic. Clinical features include dystonia, parkinsonism, ataxia, psychosis, dementia, chorea, and frontal-subcortical cognitive dysfunction. Bilateral calcifications of the basal ganglia are visualized on computed tomography (CT) scans. PFBC is genetically heterogeneous, typically inherited in an autosomal-dominant fashion. Causative mutations have been found in *SLC20A2*[2,3], which encodes the phosphate transporter PiT2[4], in *PDGFRB*[5], which encodes the platelet-derived growth factor receptor

β, and in *PDGFB*[6], which encodes the PDGFRβ main ligand. Altogether, the three genes account for 49% of PFBC families in our cohort[3].

We evaluated a North American family of Swedish ancestry with PFBC[7], lacking mutations in *SLC20A2, PDGFB*, and *PDGFRB*. Our analysis included 17 members (9 affected, 3 unaffected, and 5 individuals of unknown status, Supplementary Figure 1a). When assessed, the clinical presentation consisted of dementia, speech impairment (slurred speech, palilalia), chorea, and unsteady gait (Supplementary Table 1)[8]. CT brain scans showed extensive intracranial calcifications in basal ganglia extending to cerebral cortex or cerebellum.

Exome sequencing was performed in 4 affected (III-4, III-5, III-9, IV-6) and 1 unaffected (II-5) family members. A total of 83,848 variants were identified in the 5 samples (Supplementary Figure 1b). We first filtered out variants present in dbSNP 138 and present with a frequency >1% in the 1000 Genomes Project and Exome Variant Server databases. We then focused on missense, splice site, stop-gain/loss and frameshift variants. Seven variants (Supplementary Table 2) segregated with the disease in these five samples and were then assessed in all 17 available family members using Sanger sequencing. Only one variant was present in all affected individuals while absent in unaffected members (maximum LOD score 3.6): a c.434T>C (NM_004736.3) transition in the mammalian *xenotropic and polytropic retrovirus receptor 1* (*XPR1*) gene, predicted to induce a deleterious p.Leu145Pro change of a highly-conserved residue within the SPX domain shared by SYG1/PHO81/XPR1 proteins[9] (Fig. 1a), and absent from repositories of sequence variation, including the Exome Aggregation Consortium (ExAC) database.

Further *XPR1* sequencing in 86 additional sporadic and familial cases exposed the same p.Leu145Pro variant in two affected individuals from a family of French descent, and five additional missense variants. Pedigree analyses and segregation of variants surrounding *XPR1* suggested that the two families carrying p.Leu145Pro were not related (Supplementary Material). Three other variants, p.Ser136Asn, p.Leu140Pro and p.Leu218Ser (Table 1, Fig. 1a, Supplementary Figure 2, and Supplementary Table 3), all located in the SPX domain or in its vicinity and predicted to be damaging, were absent from variation repositories. The p.Lys53Arg variant, also absent from variation databases, is predicted to be non-damaging. The p.Ile575Val variant has a 0.068% minor allele frequency in ExAC, interchanges two hydrophobic residues in a transmembrane domain and is likely to represent a rare polymorphism. None of these variants were found in two in-house series: 126 French and 161 North-American Caucasian controls were screened with exome sequencing or targeted resequencing, respectively.

XPR1 is a cell-surface multipass membrane protein initially identified as the mammalian receptor for xenotropic-murine leukemia viruses (X-MLV)[9,10]. It contains an amino-terminal SPX domain (Fig. 1a) that is also found in several yeast and plant proteins involved in phosphate homeostasis[11,12]. We have recently shown that XPR1 mediates phosphate export[13], a function highly conserved across evolution[13,14]. We tested all the XPR1 novel variants in a complementation assay for phosphate efflux in human cells[13], wherein phosphate efflux decrease after introduction of XPR1-targeting siRNA (siXPR1) is followed

by efflux restoration upon introduction of wild type or mutated XPR1 (Fig. 1b). We found that p.Leu145Pro-mutated XPR1 neither re-established phosphate efflux, nor served as receptor for X-MLV infection (Fig. 1b and Supplementary Table 4). Consistent with this observation, phosphate efflux was also impaired in PBMC of the two patients harboring the p.Leu145Pro mutation whom we tested (Fig. 1e). This mutation affected cell surface exposure of XPR1 on HEK293T cells as monitored by flow cytometry with a XPR1 ligand (XRBD) derived from the X-MLV envelope glycoprotein[13], although the p.Leu145Pro XPR1 expression remained substantial (Fig. 1c-d). Remarkably, expression of p.Leu145Pro XPR1 specifically decreased phosphate efflux of endogenous XPR1 (Fig. 1b) while no effect on expression of phosphate importers PiT1 and PiT2 and phosphate uptake was observed (Supplementary Figure 3), supporting a trans-dominant negative effect of the p.Leu145Pro mutation on wild-type XPR1. In contrast, the four other variants were present at the plasma membrane and served as potent retroviral receptors (Supplementary Figure 4 and Supplementary Table 4). The three variants, p.Ser136Asn, p.Leu140Pro, and p.Leu218Ser, all affected XPR1 activity at various degrees, despite normal expression of the three phosphate transporters PiT1, PiT2 and XPR1 (Supplementary Figure 4). Expression of XPR1 with the predicted non-damaging p.Lys53Arg substitution restored phosphate efflux to wild-type levels, making the causative role of this variant in PFBC uncertain.

With *SLC20A2*[2,3], *XPR1* is thus the second PFBC-associated gene to encode a phosphate transporter. PFBC-causing mutations in *SLC20A2*[2,3] (PiT2) suggest that inhibition of phosphate uptake may lead to deposition of calcium phosphate in the vascular extracellular matrix. In contrast, inhibition of phosphate export, associated with the *XPR1* mutations, is expected to increase intracellular phosphate concentration. Therefore, XPR1 mutation-mediated calcium phosphate precipitation is likely to occur intracellularly, as is characteristic of osteoblasts during bone mineralization[15].

Phosphate import and export are interdependent functions that regulate intracellular phosphate homeostasis. However, it is not yet known whether XPR1 and PiT2 co-regulate each other and/or are regulated by common factors. The PFBC-associated PDGFRB and PDGFB proteins, also known to modulate phosphate transport, may also function as regulators of XPR1 and PiT2 levels in the brain[5,6,16]. PiT1 and PiT2 expression is modulated by extracellular phosphate concentration[17] and we have recently reported that high phosphate medium increases phosphate export while starvation decreases it[13]. It is therefore possible that alterations of PiT2-mediated phosphate transport may also alter XPR1-dependent phosphate export in areas of the brain where phosphate transporters are expressed[18].

Five out of six XPR1 variants described in this study are clustered in the cytoplasmic N-terminal part of XPR1 (Fig. 1a), and four lie in the SPX domain, which appears dispensable for intrinsic phosphate export activity[13]. A role of SPX in protein trafficking may explain the retention of the p.Leu145Pro XPR1 variant in cells. Interestingly, this mutation disrupts a di-leucine motif known to be involved in protein endocytosis and plasma membrane trafficking[19], and highly conserved across evolution (Supplementary Figure 5). The other mutants with impaired phosphate efflux activity were efficiently addressed to the plasma membrane, suggesting function(s) other than trafficking for the SPX domain. Thus, the SPX

domain was shown to modulate intracellular cAMP levels presumably through interactions with G protein β subunits[20], although its role in phosphate regulation remains to be elucidated.

XPR1 is actively expressed in neuronal stem cells[13], human brain[10], and in several mouse brain regions (Allen Mouse Brain Atlas database, http://mouse.brain-map.org). Direct involvement of XPR1 in phosphate export and its expression pattern in brain support its role in cerebral phosphate homeostasis. These results identify *XPR1* as a novel gene associated with PFBC and provide new insights into the role of phosphate homeostasis in PFBC etiology.

ONLINE METHODS

Patients

Patient enrollment—Seventeen individuals from one family were enrolled in this study through the UCLA Medical Center after providing informed consent. The clinical features of this family were described in a previous report[7]. Additional 86 cases self-defined as Caucasian with a clinical diagnosis of idiopathic brain calcification (either sporadic or with family history of brain calcifications) and with no mutations in *SLC20A2, PDGFB*, and *PDGFRB*, were recruited at collaborating institutions. Some of these individuals were included in previous clinical or genetic studies (47 of them were recruited using inclusion criteria as previously described[21]). The study was approved by the UCLA Institutional Review Board. Patients gave informed, written consent for genetic analyses. Medical history and neurological examinations were performed in all probands and additional family members. Serum calcium and parathormone levels were assayed to exclude calcium dysregulation and other metabolic disorders that would cause brain calcifications unrelated to PFBC.

Neuroimaging—Head computed tomography (CT scans) were performed as part of the diagnostic workup or reviewed for the presence of calcifications or other brain abnormalities. Subjects with CT scans positive for calcifications were given an affected disease status, while CT-negative patients >50 years who remained asymptomatic until their death were assigned an unaffected disease status. Subjects whose CT scans were negative but were under the age of 50, or whose CT scan results were not available, were classified as unknown.

Exome analysis

Genomic DNA was extracted from peripheral blood and fragmented by sonication using the Covaris acoustic disruptor (E210, Covaris Inc.) to achieve an average fragment size of 200 base pairs. One microgram of DNA from each individual was used for the construction of a paired-end library, exome capture was performed using the TruSeq DNA Sample Prep Kit (Illumina).

Sequencing was performed on an Illumina Genome Analyzer HiSeq2500 following the manufacturer’s instructions. 46.4 million 100-base, paired-end reads were obtained per sample on average, with a 20x average depth of coverage within the targeted exome. Raw

image files were processed with the Illumina CASAVA 1.8 software (Illumina). The sequencing reads were aligned to the National Center for Biotechnology Information human reference genome (GRCh37/hg19) using the Burrows-Wheeler Aligner (BWA). Variant calling was performed using Genome Analysis Toolkit (GATK, version 2.6.4) and QIAGEN's Ingenuity Variant Analysis™ software (QIAGEN) was used for variants annotation and filtering. Filtration was carried out applying a series of steps (Supplementary Figure 1b): low-quality variants were filtered out using the Illumina Qscore threshold of 20; in addition, variants present in dbSNP138 and with a minor allele frequency (MAF) higher than 1% in the 1000 Genomes Project data (http://www.1000genomes.org/) and Exome Variant Server (EVS, http://evs.gs.washington.edu/EVS/) databases were filtered out; finally, we focused on predicted missense, frameshift, stop gain/loss, and splice-site variants. The potential effect of the variants on the protein function was assessed by Polyphen2, SIFT and Mutation Taster. Polyphen2 is a software tool that predicts damaging effects combining an evaluation of the properties of the mutated amino acid and of the conservation of the residue[22]. SIFT is a tool developed to predict the deleterious effect of an amino acid substitution basing on sequence homology analysis[23]. Mutation Taster is a web-based application that integrates information from several analysis tools. The disease potential is evaluated comprising analysis on evolutionary conservation, splice-site changes, loss of protein features and changes that might affect the amount of mRNA[24]. Residue conservation was evaluated using the Genomic Evolutionary Rate Profiling (GERP), an algorithm that identifies constrained elements in multiple alignments by quantifying substitution deficits[25]. GERP score ranges from –12.3 to 6.17, with 6.17 being the most conserved elements. Protein schematic (Fig. 1a) was created using TOPO2, Transmembrane protein display software (http://www.sacs.ucsf.edu/TOPO2). Variant frequency was also checked in Exome Aggregation Consortium (ExAC), database, Cambridge, MA (URL: http://exac.broadinstitute.org) [accessed February 2015], where *XPR1* has a mean coverage = 65.2x (range: 41–206x) across 115,519.9 alleles on average.

Sanger Sequencing analysis

Sanger sequencing was initially performed to screen the genes already known to be associated with PFBC (i.e. *SLC20A2, PDGFRB, PDGFB*) and to validate the variants identified through exome sequencing. Genomic DNA extracted from the blood was used as template for PCR reactions in order to amplify the coding regions of *SLC20A2* (NM_001257180.1), *PDGFB* (NM_002608.2) and *PDGFRB* (NM_002609.3), as well as that of *XPR1* (NM_004736.3), focus of this study.

Cosegregation analysis

The maximum LOD score (recombination rate = 0) was computed assuming an autosomal dominant pattern of inheritance, a penetrance of 100% at age 50 (12 informative meioses fulfilling these criteria), according to the formula $Z(\theta) = \log[(1-\theta)^{n-r}\,\theta^{r}/(1/2)^{n}]$, where n = total number of births, r = number of recombinant types, and θ = recombination rate.

Analysis of relatedness between the two families carrying the c.434T>C, p.Leu145Pro *XPR1* variant

We studied the genealogy of both families whose members included carriers of the c. 434T>C, p.Leu145Pro variant. We obtained data up to the 1750s in one branch of the French family (mother of the proband, known to be affected) and could not find any common ancestry with the North-American family of Swedish descent. Furthermore, we compared exome sequencing from all affected and unaffected individuals from the North-American family in *XPR1* and the surrounding genes on chromosome 1, and identified three variants (one downstream and two upstream of *XPR1*) that were present in affected and absent in the unaffected individual: rs7536561 (529 kb from the *XPR1* variant), rs79485039 (113 kb from the *XPR1* variant), and rs3747958 (125 kb from the *XPR1* variant). We sequenced these SNPs in the proband of the French family who also carried the c.434T>C, p.Leu145Pro mutation and found reference sequences for all of them. This supported the hypothesis that the mutation occurred on different haplotypes in the two families.

Cells

HEK293T (human embryonic kidney) and CHO hamster cells were cultured in DMEM supplemented with 10% fetal bovine serum (FBS, Invitrogen) and non-essential amino acids, in a 5% CO2 incubator at 37°C under humid atmosphere. For phosphate-free incubations, cells were grown in phosphate-free DMEM supplemented with 10% dialysed FBS.

Peripheral blood mononuclear cells (PBMC) were isolated from peripheral blood collected in presence of heparin from both healthy donors and patients who have signed informed consent for research purposes. Blood samples were subjected to density gradient separation on Histopaque-1077 (ratio 1:1) (Sigma-Aldrich) and centrifuged 24 hours after blood collection. After centrifugation, the PBMC layer was collected and washed in DMEM before evaluation of phosphate efflux.

Plasmids and siRNAs

The p.Leu145Pro, p.Lys53Arg, p.Ser136Asn, p.Leu140Pro and p.Leu218Ser mutations were generated by site-directed mutagenesis using recombinant PCR (details are available upon request). The HA-tagged versions of human XPR1 were introduced in both the pCHIX expression vector[26] and pLXSN retroviral vector[27]. Sequences of small interfering RNAs (siRNA, Integrated DNA Technologies) targeting the 3' UTR of human *XPR1* were as follows: 5'-ggauuucaugccaucccautt-3' and 5'-gcacuuccaccauguauuatt-3'. siRNA directed against the *firefly luciferase* gene was used as control. HEK293T cells grown on poly-D-lysine coated 6-well plates were transfected with 50 pmol siRNA per well using the calcium phosphate method.

^{33}Phosphate fluxes in human cells

Phosphate uptake and efflux from HEK293T cell monolayers transfected 2 days prior to assays were measured as previously described[9]. Briefly, for uptake measurements, cells were incubated 30 min at 37°C in phosphate-free DMEM supplemented with 0.5μCi/ml

[^{33}P]phosphate (NEZ080500UC, Perkin Elmer). Cell lysates were then assayed for radioactivity by scintillation counting and for protein content by the BCA protein assay (Pierce). The percentage of phosphate uptake was calculated as the ratio of cellular [^{33}P]phosphate to total [^{33}P]phosphate supplemented. For the efflux measurements, cells were incubated 20 min at 37°C in phosphate-free DMEM supplemented with 0.5μCi/ml [^{33}P]phosphate (NEZ080500UC, Perkin Elmer), gently washed three times with phosphate-free medium and then incubated in DMEM for 30 min at 37°C in 10mM phosphate before collecting the supernatant. [^{33}P]phosphate in the supernatants and cell lysates was measured by liquid scintillation. The percentage of phosphate efflux was calculated as the ratio of released [^{33}P]phosphate to total cellular [^{33}P]phosphate. Phosphate efflux in PBMC was assayed as described above with 0.5×10^6 cells per assay.

Immunoblotting

Whole cell extracts (15μg) were analyzed on 12% SDS-PAGE under reducing conditions, transferred to PVDF membranes and probed with antibodies against HA (3F10, 1:5000, Roche Applied Science) or β-actin (A5441, 1:5000, Sigma-Aldrich). Proteins of interest were detected with horseradish peroxidase-conjugated anti-mouse or anti rat antibodies (1:5000, SouthernBiotech) and visualized with the Pierce ECL Western blotting substrate (Thermo Scientific), according to the manufacturer's protocol.

Flow Cytometry

Cell surface expression of phosphate transporters was monitored on HEK293T cells with soluble ligands derived from the receptor-binding domain (RBD) of different Env. Xenotropic-MLV RBD (XRBD), koala retrovirus (KoRV) RBD (KoRBD) and amphotropic-MLV RBD (ARBD) were used to detect XPR1, PiT1 and PiT2[13,28], respectively. Binding assays were carried out as previously described[13]. Briefly, 5×10^5 cells were resuspended in 200μl PBA (PBS with 2% FBS and 0.1% sodium azide) containing the proper RBD, incubated for 30 min at 37°C, washed twice with PBA and incubated for 20 min at 4°C with Alexa488-conjugated anti-mouse IgG1 antibodies (1/500 dilution, Invitrogen). Cells were immediately analyzed on a FACSCalibur (Becton Dickinson) and data analysis was performed using FlowJo software.

Virus production

LAPSN virus vectors were produced in 2×10^6 HEK293T cells in 10 cm dishes cotransfected using calcium phosphate with the MLV-based LAPSN retroviral vector carrying the *alkaline phosphatase* reporter gene[29] (10μg), the MLV Gag/Pol expression vector (pC57GPBEB, 5μg)[30], and either the vesicular stomatitis virus (VSV) G protein or the X-MLV envelope glycoprotein (Env) expression vectors (5μg). Virion-containing media were harvested 2 days later, filtered through 0.45 μm (pore size) filter and stored at -80°C before use. LXSN virus vectors carrying wild type and mutated *XPR1* genes were produced in the same conditions except that the LAPSN retroviral vector was replaced by the various XPR1 LXSN vectors.

Viral Infection and G418 selection

CHO cells stably expressing XPR1 constructs were generated by transducing CHO cells with the pL(XPR1)SN, pL(XPR1K53R)SN, pL(XPR1S136N)SN, pL(XPR1L140P)SN, pL(XPR1L145P)SN, pL(XPR1L218S)SN or empty pLXSN vectors and selected the next day with medium containing 1.5 mg per ml of G418 (active fraction). G418-resistant clones were pooled after 2 weeks of selection before further experiments.

2×10^4 hamster CHO cells, stably expressing wild type, p.Lys53Arg, p.Ser136Asn, p.Leu140Pro, p.Leu145Pro or p.Leu218Ser XPR1 from the MLV-based retroviral vector LXSN, were plated in 12-well plates and infected the following day with serial dilutions of replication-defective LAPSN retroviral vector pseudotyped with X-MLV Env or the VSV-G glycoprotein. Cells were stained 2 days later for alkaline phosphatase (AP) expression, as previously described[29], and AP-positive colonies were counted to determine viral titers (colony forming units per ml).

Statistical analysis

The Student's *t* test in GraphPad Prism 5 software (GraphPad) was used to calculate *P* values, and the following convention was used: *$P\leq0.05$; ** $P\leq0.01$; *** $P\leq0.001$; **** $P\leq0.0001$.

Supplementary Material

Refer to Web version on PubMed Central for supplementary material.

Acknowledgments

We would like to acknowledge and thank all of the participants and families for their valuable contribution to our study; our clinical staff and laboratory members, Joseph DeYoung and the UCLA Neuroscience Genomics Core, J. Touhami and J. Laval for their assistance and constant support; the NHLBI GO Exome Sequencing Project and its ongoing studies, which produced and provided exome variant calls for comparison: the Lung GO Sequencing Project (HL-102923), the WHI Sequencing Project (HL-102924), the Broad GO Sequencing Project (HL-102925), the Seattle GO Sequencing Project (HL-102926) and the Heart GO Sequencing Project (HL-103010). We are also indebted to the Montpellier Rio Imaging (MRI) platform for flow cytometry experiments. This work was funded by NIH/NINDS (R01 NS040752 to DHG), by Association Française contre les Myopathies (AFM) and Ligue Nationale contre le Cancer (Comité de l'Hérault) (to JLB), and by *Fondation pour la Recherche Medicale* (FRM) and a FEDER European Union-Languedoc-Roussillon grant (*Transportome*) (to MS). DG was supported by FRM, INCa and Labex GR-Ex (ANR-11-LABX-0051) fellowships and ULS by a Labex EpiGenMed (ANR-10-LABX-12-01) fellowship; Labex is funded by the program '*Investissements d'Avenir*" of the French National Research Agency; JLB and MS were supported by INSERM; MJS and BQ are supported by the Fondo de Investigación Sanitaria, grant PI12/00742; INNOPHARMA project MINECO-USC and FEDER funds; MJS and BQ hold research contracts from the Institute of Health Carlos III - SERGAS; JRMO acknowledges funding from FACEPE (APQ 1831-4.01/12) and CNPq (457556/2013-7;480255/2013-0; 307909/2012-3). BLF is funded by NIH Grants K08MH086297 (NIMH) and R01NS082094 (NINDS). GN, ACR, DH, and DC are supported by INSERM, the University Hospital of Rouen and the French CNR-MAJ.

References

1. Sobrido, MJ., et al. GeneReviews. Pagon, RA., et al., editors. Seattle: University of Washington; 2013. 1993–2015 URL (www.ncbi.nlm.nih.gov/books/NBK1421)
2. Wang C, et al. Nat. Genet. 2012; 44:1098–1103. [PubMed: 22922876]
3. Hsu SC, et al. Neurogenetics. 2013; 14:11–22. [PubMed: 23334463]
4. Kavanaugh MP, et al. Proc. Natl. Acad. Sci. USA. 1994; 91:7071–7075. [PubMed: 8041748]

5. Nicolas G, et al. Neurology. 2013; 80:181–187. [PubMed: 23255827]
6. Keller A, et al. Nat. Genet. 2013; 45:1077–82. [PubMed: 23913003]
7. Boller F, Boller M, Gilbert J. J. Neurol. Neurosurg. Psychiatry. 1977; 40:280–5. [PubMed: 886353]
8. Oliveira J, et al. Neurology. 2004; 63:2165–2167. [PubMed: 15596772]
9. Battini JL, Rasko JE, Miller AD. Proc. Natl. Acad. Sci. USA. 1999; 96:1385–1390. [PubMed: 9990033]
10. Tailor CS, Nouri A, Lee CG, Kozak C, Kabat D. Proc. Natl. Acad. Sci. USA. 1999; 96:927–32. [PubMed: 9927670]
11. Secco D, et al. New. Phytol. 2012; 193:842–851. [PubMed: 22403821]
12. Secco D, Wang C, Shou H, Whelan J, et al. FEBS Lett. 2012; 586:289–295. [PubMed: 22285489]
13. Giovannini D, Touhami J, Charnet P, Sitbon M, Battini JL, et al. Cell Rep. 2013; 3:1866–1873. [PubMed: 23791524]
14. Wege S, Poirier Y, et al. FEBS Lett. 2014; 588:482–489. [PubMed: 24374333]
15. Boonrungsiman S, et al. Proc. Natl. Acad. Sci. USA. 2012; 109:14170–14175. [PubMed: 22879397]
16. Kakita A, et al. Atherosclerosis. 2004; 174:17–24. [PubMed: 15135246]
17. Kavanaugh MP, Kabat D, et al. Kidney Int. 1996; 49:959–963. [PubMed: 8691744]
18. Lagrue E, et al. J. Biomed. Sci. 2010; 17:91. [PubMed: 21129221]
19. Guo Y, Jose PE, et al. PLOS One. 2011; 6:e29204. [PubMed: 22206002]
20. Vaughan AE, Mendoza R, Aranda R, Battini JL, Miller AD, et al. J. Virol. 2012; 86:1661–1669. [PubMed: 22090134]

Supplementary References

21. Nicolas G, et al. P Brain. 2013; 136:3395–3407.
22. Adzhubei IA, et al. Nat. Methods. 2010; 7:248–249. [PubMed: 20354512]
23. Ng PC, Henikoff S. Genome Res. 2001; 11:863–874. [PubMed: 11337480]
24. Schwarz JM, Rödelsperger C, Schuelke M, Seelow D. Nat. Methods. 2010; 7:575–576. [PubMed: 20676075]
25. Cooper GM, et al. Genome Res. 2005; 15:901–913. [PubMed: 15965027]
26. Manel N, et al. Cell. 2003; 115:449–459. [PubMed: 14622599]
27. Miller AD, Rosman GJ. Biotechniques. 1989; 7:980–982. 984–986, 989–990. [PubMed: 2631796]
28. Petit V, et al. Lab. Invest. 2013; 93:611–621. [PubMed: 23459372]
29. Miller DG, Edwards RH, Miller AD. Proc. Natl. Acad. Sci. USA. 1994; 91:78–82. [PubMed: 8278411]
30. Lassaux A, Sitbon M, Battini J-L. J. Virol. 2005; 79:6560–6564. [PubMed: 15858043]

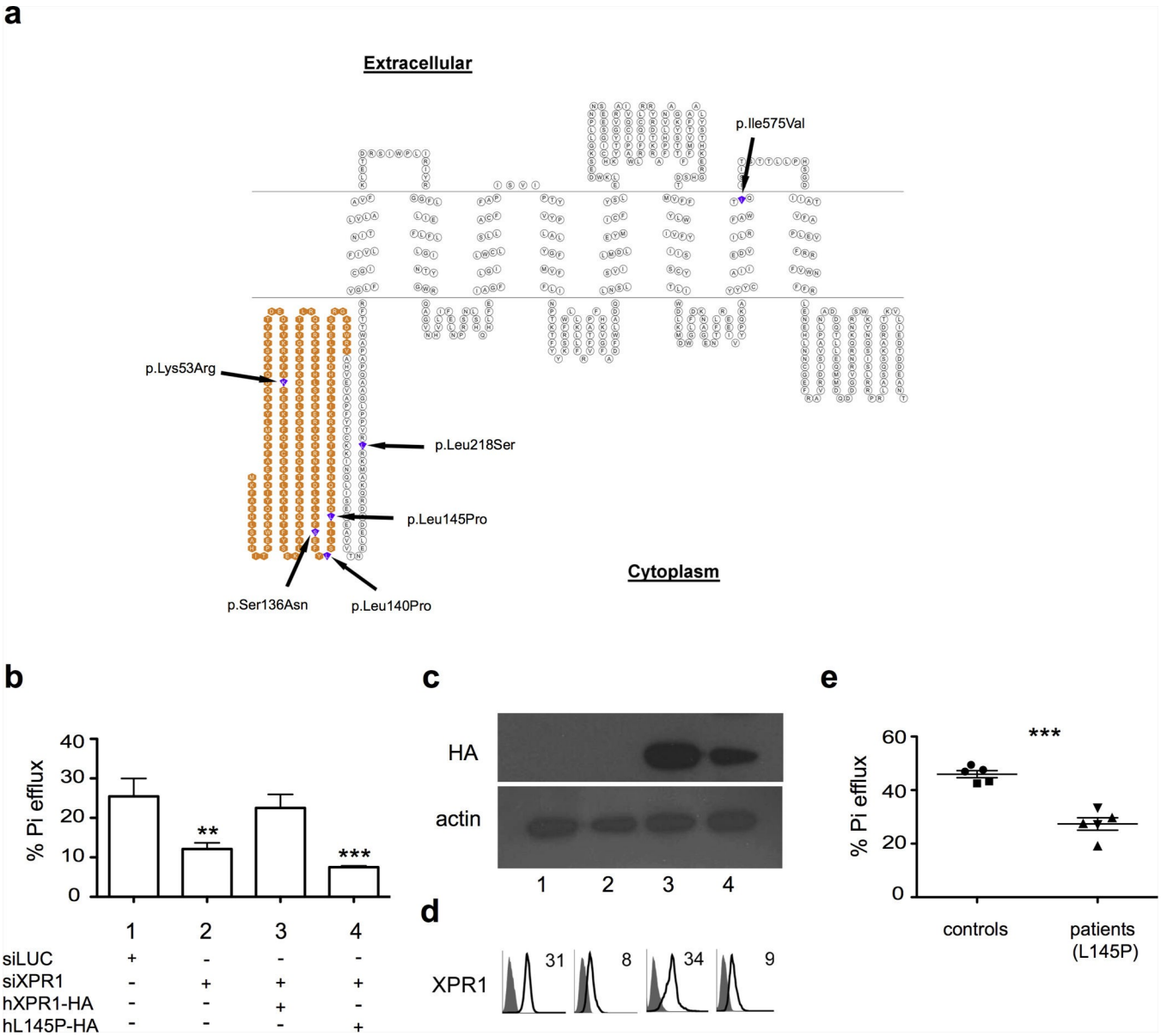

Figure 1. Localization of the Variants Identified in the XPR1 Protein and Effect of the p.Leu145Pro on Protein Expression and Function

(**a**) Schematic representation of the XPR1 protein and the variants identified in this study. The SPX domain is in orange. (**b**) Efflux of inorganic ^{33}P in HEK293T cells transfected with siLUC (Lane 1), siXPR1 alone (Lane 2) or in combination with HA-tagged wild type (Lane 3) or p.Leu145Pro XPR1 (Lane 4). Results are means ± s.e.m. in a representative experiment (n=3); $^{**}P \leq 0.01$ and $^{***}P \leq 0.001$ as tested against siLUC. (**c**) Immunoblot of HA-tagged XPR1 expression in cell lysates with an anti-HA antibody (upper panel). β-actin was used as loading control (lower panel). (**d**) Cell-surface detection of XPR1 on HEK293T cells transfected as in (b). Nonspecific staining with the secondary IgG antibody (filled histograms) and specific binding with X-MLV RBD (solid line histograms) are represented. Numbers indicate specific mean fluorescence intensity of a representative experiment (n=3).

(**e**) Efflux of ^{33}P in PBMC collected from two control healthy donors (each symbolized by circles or squares), and two affected patients harboring the p.Leu145Pro mutation (each symbolized by triangles pointing up or down). Bars represent means ± s.e.m., ***P ≤ 0.001.

Table 1

Rare Variants Identified In *XPR1* in the Proband and a Cohort of 86 Index Cases.

Genomic Position	cDNA	Protein	PolyPhen-2 Function Prediction	SIFT Function Prediction	MutationTaster Function Prediction	dbSNP ID	1KGP Frequency	NHLBI EVS Frequency	ExAC Allelic Frequency	GERP
chr1:180756925	c.158A>G	p.Lys53Arg	Benign	Tolerated	Disease causing	-	absent	absent	absent	5
chr1:180772707	c.407G>A	p.Ser136Asn	Probably Damaging	Damaging	Disease causing	-	absent	absent	absent	5.93
chr1:180772719	c.419T>C	p.Leu140Pro	Probably Damaging	Damaging	Disease causing	-	absent	absent	absent	5.93
chr1:180772734	c.434T>C	p.Leu145Pro	Probably Damaging	Damaging	Disease causing	-	absent	absent	absent	5.93
chr1:180775665	c.653T>C	p.Leu218Ser	Probably Damaging	Damaging	Disease causing	-	absent	absent	absent	5.15
chr1:180842993	c.1723A>G	p.Ile575Val	Benign	Tolerated	Disease causing	rs147941113	0.040%	0.054%	83/121,330 (0.068%)	2.09

1KGP: 1000 Genomes Project (http://www.1000genomes.org/)

NHLBI EVS: NIH Heart, Lung, and Blood Institute Exome Variant Server (EVS, http://evs.gs.washington.edu/EVS/)

ExAC: Exome Aggregation Consortium database, Cambridge, MA (URL: http://exac.broadinstitute.org) [accessed February 2015]

Variants in *XPR1* currently explain about 5.5% in the French cohort, and 2.5% in the North American cohort. Thus, *XPR1* mutations are less common than *SLC20A2* and *PDGFB*, but more common than *PDGFRB*.